D J Med Sci 2025;11(3):134-143
doi: 10.5606/fng.btd.2025.208

Original Article

Integrative meta-analysis reveals coordinated H19/miR-675/circRNA network remodeling and metabolic reprogramming in tamoxifen-treated MCF-7 cells

Elif Yorgun, Özge Acar

Department of Genetics and Bioenginnering, İstanbul Okan University, İstanbul, Türkiye

ABSTRACT

Objectives: This study aimed to identify transcriptomic signatures associated with established tamoxifen resistance in ER-positive MCF-7 cells through integrative meta-analysis of public datasets and to evaluate whether H19-centered non-coding RNA networks constitute early adaptive transcriptional responses following acute tamoxifen exposure.

Materials and methods: We interrogated three publicly available transcriptomic datasets (GSE67916, GSE26459, GSE5840) comprising 32 biological samples from tamoxifen-resistant and parental MCF-7 cells using the ImaGEO analytical framework. Pathway-level characterization was achieved via Gene Ontology, Kyoto Encyclopedia of Genes and Genomes, and Reactome enrichment pipelines. To corroborate computational predictions, we quantified transcript abundance of lncRNA H19, miR-675-5p, circRNA sponge for miR-7 (ciRS-7), and circRNA homeodomain-interacting protein kinase 3 (circHIPK3) using quantitative polymerase chain reaction following a 48-h tamoxifen challenge at the experimentally derived IC_{50} (5 μM).

Results: Computational screening unveiled 2,096 transcripts exhibiting consistent expression alterations (false discovery rate (FDR) <0.05), comprising 1,180 induced and 916 repressed genes. Pathway mapping revealed pronounced activation of the cholesterol synthesis machinery and sterol regulatory element-binding protein-driven transcriptional circuits, along with enhanced immunological signatures, in resistant cells. Conversely, genes governing mitochondrial protein synthesis and forkhead-box class O/Hippo tumor-suppressive cascades showed marked attenuation. Laboratory validation demonstrated coordinate elevation of H19, miR-675-5p, and ciRS-7 transcripts, while circHIPK3 levels declined substantially upon tamoxifen challenge (all p<0.001).

Conclusion: This investigation uncovers synchronized alterations in lipid metabolic programming and the H19/miR-675/circRNA regulatory axis triggered by tamoxifen exposure. Our observations illuminate molecular perturbations that may foreshadow the emergence of treatment-refractory disease and highlight candidate nodes warranting therapeutic exploration in hormone-dependent breast malignancies.

Keywords: Breast carcinoma, competing endogenous RNA, endocrine resistance, H19 long non-coding RNA, miR-675.

Breast cancer remains the most frequently diagnosed malignancy among women worldwide and represents a major cause of cancer-related mortality. Statistical projections from 2022 documented roughly 2.3 million incident cases alongside more than 666,000 fatalities attributable to this disease.[1] The majority of breast tumors, which are estimated between 70 and 80 percent, harbor estrogen receptor (ER) expression, rendering hormonal intervention the therapeutic mainstay for this molecular subset.[2] Tamoxifen, functioning as a selective modulator of ER activity, has anchored clinical management protocols spanning four decades. Nevertheless, a substantial fraction of patients, ranging from 30 to 50 percent, ultimately develop therapeutic refractoriness, leading to disease progression and clinical deterioration.[3,4]

The biological underpinnings of tamoxifen unresponsiveness encompass multifaceted alterations, including perturbations in receptor signaling, compensatory engagement of growth factor pathways, and cellular metabolic rewiring.[5] Contemporary investigations have underscored the role of sterol homeostatic mechanisms in contributing to endocrine treatment failure. Transcriptional

Received: January 03, 2026
Accepted: January 19, 2026
Published online: January 28, 2026

Correspondence: Elif Yorgun.
E-mail: elif.yorgun@okan.edu.tr

Cite this article as:
Yorgun E, Acar Ö. Integrative meta-analysis reveals coordinated H19/miR-675/circRNA network remodeling and metabolic reprogramming in tamoxifen-treated MCF-7 cells. D J Med Sci 2025;11(3):134-143. doi: 10.5606/fng.btd.2025.208.

programs orchestrated by sterol regulatory element-binding protein (SREBP) facilitate neoplastic cell persistence under therapeutic pressure.[6,7] Concurrently, compromised mitochondrial integrity coupled with attenuated tumor-suppressive circuitry, notably forkhead-box class O (FoxO) and Hippo signaling pathway components, has emerged as a mechanistic contributor to resistant phenotypes.[2] These collective observations implicate metabolic plasticity as a cornerstone of tamoxifen resistance biology, necessitating deeper interrogation of the regulatory architectures that govern it.

The regulatory landscape of therapeutic resistance increasingly implicates non-protein-coding transcripts. The developmentally regulated long non-coding RNA (lncRNA) H19 participates in tamoxifen refractoriness through autophagy induction and epigenetic modulation of N-acetyltransferase 1 locus methylation.[8,9] Beyond its autonomous functions, H19 serves as the genomic template for microRNA (miR)-675 biogenesis, a miRNA that promotes tumor growth via post-transcriptional silencing of the E3 ubiquitin ligases c-Cbl and Cbl-b, thereby perpetuating receptor tyrosine kinase activation.[10] Additionally, H19 may interact with circular RNAs (circRNAs) via shared miRNA response elements within competing endogenous RNA (ceRNA) frameworks. The circular transcript circRNA sponge for miR-7 (ciRS-7, also designated cerebellar degeneration-related protein 1 antisense; CDR1as), established as a molecular decoy for miR-7, promotes malignant progression across diverse tumor histologies,[11] whereas circRNA homeodomain-interacting protein kinase 3 (circHIPK3) contributes to chemotherapeutic resistance through autophagy-linked mechanisms.[4] The concurrent perturbation of these regulatory transcripts in treatment-refractory contexts underscores the imperative to examine them in an integrated manner.

The present investigation employed a systematic integration of publicly archived transcriptomic repositories from tamoxifen-resistant Michigan Cancer Foundation-7 (MCF-7) populations to delineate consistently perturbed genetic elements associated with hormonal resistance. Functional annotation pipelines characterized aberrant biological processes and signaling conduits. Computational outputs revealed metabolic restructuring alongside post-transcriptional network disturbances. Informed by these discoveries, we prioritized the H19/miR-675 regulatory module, together with ciRS-7 and circHIPK3, for empirical verification via quantitative amplification assays following tamoxifen challenge. Importantly, whereas our computational framework captures molecular signatures of established resistance, our laboratory experiments probe acute transcriptional responses to immediate drug exposure, potentially reflecting adaptive precursors antecedent to overt resistance consolidation.

MATERIALS AND METHODS

Transcriptomic data acquisition

Expression profiling datasets of tamoxifen responsiveness in MCF-7 breast adenocarcinoma cells were retrieved from the National Center for Biotechnology Information Gene Expression Omnibus (GEO) repository. Dataset inclusion required satisfaction of predetermined criteria: *(i)* utilization of MCF-7 human mammary carcinoma cells, *(ii)* parallel profiling of tamoxifen-resistant alongside sensitive or untreated counterparts, and *(iii)* accessibility of processed quantitative data amenable to cross-study integration.

All incorporated datasets were derived from oligonucleotide microarray platforms. Transcript identifiers were harmonized to the standardized HUGO Gene Nomenclature Committee (HGNC) nomenclature prior to analytical workflows. The analytical corpus comprised GSE67916 (18 specimens: 8 parental, 10 resistant), GSE26459 (6 specimens: 3 parental, 3 resistant), and GSE5840 (8 specimens: 4 parental, 4 resistant), collectively representing 32 biological samples.

Computational analytical framework

Cross-study expression integration

Multi-dataset expression synthesis was executed through the ImaGEO computational interface,[12] engineered to amalgamate transcriptomic outputs spanning independent investigations. Within individual datasets, comparative expression profiling contrasting

resistant versus sensitive MCF-7 populations employed statistical algorithms native to the platform.

Cross-study consistency was assessed via Z-score aggregation methodology, accommodating inter-study heterogeneity. Resultant probability values underwent multiple comparison adjustment through Benjamini-Hochberg false discovery rate correction. Transcripts achieving adjusted significance thresholds (false discovery rate (FDR) <0.05) were designated meta-differentially expressed genes (meta-DEGs). Directional classification employed Z-score polarity: positive values indicated transcriptional induction, whereas negative values denoted repression in resistant populations.

Meta-DEG refinement procedures

Platform-generated meta-DEG inventories underwent systematic curation antecedent to pathway interrogation. Multi-symbol entries were disaggregated into discrete gene records. Duplicate identifiers were resolved through retention of entries bearing minimal FDR values. Transcripts lacking validated or mappable identifiers were excluded from downstream pathway analyses. Induced and repressed transcript populations underwent segregated analytical processing throughout subsequent workflows.

Functional ontology assessment

Gene Ontology (GO) categorization employed the clusterProfiler analytical suite (release 4.8.3) within the R computational environment. Symbol-to-identifier conversion utilized the org.Hs.eg.db annotation resource (release 3.18.0), with successfully mapped transcripts proceeding to enrichment testing. Biological Process (BP) ontology terms underwent hypergeometric evaluation with Benjamini-Hochberg adjustment, accepting terms satisfying adjusted significance criteria ($p<0.05$).

KEGG pathway mapping

Kyoto Encyclopedia of Genes and Genomes (KEGG) pathway enrichment analysis was performed using the enrichKEGG function implemented in the clusterProfiler package (release 4.8.3). Upregulated and downregulated gene assemblies underwent independent pathway assessment utilizing Entrez numerical identifiers. Pathways achieving adjusted significance (Benjamini-Hochberg correction; $p<0.05$) were deemed enriched, with graphical visualization through dot plot representations.

Reactome database interrogation

Reactome pathway evaluation utilized the ReactomePA analytical package (release 1.44.0). Segregated analysis of induced versus repressed meta-DEGs identified overrepresented pathways catalogued within the Reactome knowledgebase. Statistical significance employed hypergeometric probability assessment with Benjamini-Hochberg correction, accepting pathways meeting adjusted thresholds ($p<0.05$).

Statistical computing environment

Computational analyses were conducted within the R statistical framework (release 4.3.2). Multiple testing adjustment consistently employed Benjamini-Hochberg methodology across all enrichment assessments, with significance established at adjusted probability thresholds below 0.05.

Laboratory experimental procedures

Cellular viability assessment

Tamoxifen cytotoxicity profiling in MCF-7 populations employed colorimetric viability quantification. Cells were distributed into 96-well formats at 5×10^3 cells per well in complete propagation medium, permitting 24-h adhesion. Subsequently, escalating tamoxifen concentrations (0, 1.5625, 3.125, 6.25, 12.5, 25, 50, and 100 μM) were administered in triplicate configurations. Following 48-h incubation, viability was quantified via Cell Counting Kit-8 (CCK-8) methodology per manufacturer specifications: 10 μL reagent addition preceded 2-h chromogenic development at 37 °C, with spectrophotometric detection at 450 nm.

Half-maximal inhibitory concentration derivation

Viability percentages were computed relative to vehicle-treated populations. Concentration-response relationships were modeled through GraphPad Prism (release 8.0) nonlinear

regression algorithms. The IC_{50}-defined as the tamoxifen concentration affecting 50% viability reduction-was extrapolated from fitted curves, yielding 5 µM as the working concentration for subsequent molecular investigations.

Cell propagation and pharmacological challenge

The MCF-7 mammary carcinoma cells (ATCC® HTB-22™) were propagated in high-glucose Dulbecco's Modified Eagle Medium supplemented with 10% fetal bovine serum and 1% antimicrobial formulation, maintained at 37 °C under 5% CO_2 humidification. Experimental populations underwent seeding followed by 24-h attachment. Tamoxifen was introduced at the empirically determined IC_{50} (5 µM) for 48-h exposure periods, with parallel control populations receiving vehicle (0.1% dimethyl sulfoxide) under equivalent conditions.

Nucleic acid isolation and reverse transcription

Total RNA procurement employed the miRNeasy Tissue/Cells Advanced isolation system (Qiagen, Hilden, Germany) following manufacturer protocols. RNA quantity and purity underwent spectrophotometric verification, with integrity confirmation preceding downstream applications. For lncRNA and messenger RNA targets, 500 ng template underwent reverse transcription via RT2 First Strand reagents (Qiagen, Hilden, Germany). MicroRNA conversion employed miRCURY LNA RT chemistry (Qiagen, Hilden, Germany) per supplied instructions.

Quantitative transcript amplification

Real-time quantitative amplification utilized SYBR Green fluorescence chemistry. Individual reactions comprised 20 µL volumes containing template, sequence-specific oligonucleotides, and detection master mix, performed in technical triplicate. All primers used in this study were selected based on previously published literature, and their corresponding amplicon sizes are presented in Table 1. Thermal cycling consisted of an initial denaturation step followed by 40 amplification iterations. Oligonucleotide sequences targeting analytical transcripts (lncRNA H19, miR-675-5p, ciRS-7, circHIPK3) alongside reference sequences (ACTB, U6) are provided in Table 1. Amplification fidelity was verified through dissociation curve profiling.

Transcript abundance underwent normalization against ACTB (lncRNA/mRNA targets) or U6 (miRNA targets) housekeeping transcripts. Relative expression alterations between experimental and control cohorts were computed via the $2^{-}\Delta\Delta Ct$ algorithm, expressed as fold modulation relative to untreated populations.

This study did not involve human participants or animal experiments and therefore did not require ethical approval.

Table 1. Primer sequences for qPCR reactions

Primer name	Sequence	Amplicon size (bp)	Reference
ACTB_F	CACCATTGGCAATGAGCGGTTC	135	Literature-based
ACTB_R	AGGTCTTTGCGGATGTCCACGT		Literature-based
U6-snRNA_F	CTCGCTTCGGCAGCACA	94	Literature-based
U6-snRNA_R	AACGCTTCACGAATTTGCGT		Literature-based
H19_F	CGTCCGGCCTTCCTGAACA	149	Literature-based
H19_R	TTGAGCTGGGTAGCACCATTTCT		Literature-based
hsa-miR-675-5p_F	TTGGTGGTGCGGAGAG	86	Literature-based
hsa-miR-675-5p_R	AGTGCGTGTCGTGGAGTC		Literature-based
circHIPK3_F	CCAGTGACAGTTGTGACAGCTACC	147	Literature-based
circHIPK3_R	GCCAAACGTGCCTCGACCAAG		Literature-based
ciRS-7_F	ACGTCTCCAGTGTGCTGA	90	Literature-based
ciRS-7_R	CTTGACACAGGTGCCATC		Literature-based

qPCR: Quantitative polymerase chain reaction. All primers were literature-based and synthesized commercially.

Statistical analysis of qPCR data

All quantitative polymerase chain reaction (qPCR) experiments were performed in three independent biological replicates. Data are presented as mean ± standard deviation (SD). Statistical differences between groups were assessed using an unpaired two-tailed Student's t-test, with $p<0.05$ considered statistically significant.

RESULTS

Integrated transcriptomic analyses reveal coordinated metabolic and signaling alterations associated with tamoxifen resistance

To delineate transcripts that reproducibly associate with tamoxifen unresponsiveness in MCF-7 mammary carcinoma populations, we conducted systematic integration across multiple independent GEO repositories using the ImaGEO analytical framework. Following false discovery correction, 2,096 meta-differentially expressed transcripts were identified (FDR <0.05), encompassing 1,180 induced and 916 repressed transcripts in treatment-refractory versus treatment-sensitive counterparts. This integrative methodology attenuated dataset-specific confounding while enabling robust identification of transcriptional perturbations underlying endocrine resistance.

Gene Ontology Biological Process categorization was independently applied to induced and repressed meta-DEG populations. Among upregulated transcripts, pronounced overrepresentation was observed in lipid

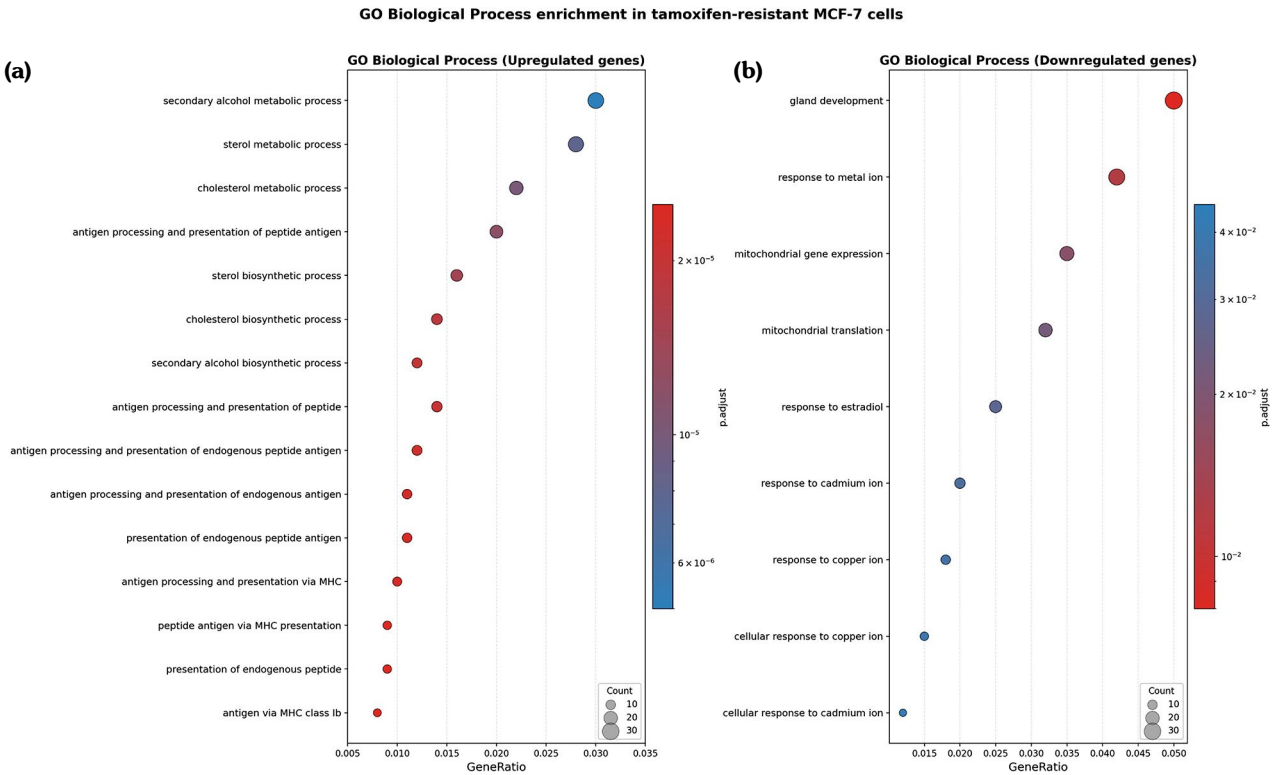

Figure 1. Gene Ontology (GO) Biological Process enrichment analysis of meta-differentially expressed genes associated with tamoxifen resistance. Dot plots show significantly enriched Gene Ontology Biological Process (BP) terms for upregulated **(a)** and downregulated **(b)** meta-differentially expressed genes identified by ImaGEO-based meta-analysis of MCF-7 tamoxifen-resistant datasets. Dot size represents the number of genes associated with each GO term, while color intensity indicates the adjusted p-value (Benjamini-Hochberg correction). Upregulated genes are predominantly enriched in lipid and sterol metabolic processes as well as antigen processing and presentation pathways. In contrast, downregulated genes are mainly associated with mitochondrial translation, mitochondrial gene expression, and estrogen-responsive biological processes.

MCF-7: Michigan Cancer Foundation-7; ImaGEO: Gene Expression Omnibus.

and sterol metabolic processes-specifically, secondary alcohol metabolism, sterol homeostasis, cholesterol metabolism, and cholesterol biosynthetic cascades, as shown in Figure 1a. Simultaneously, immunological processes achieved significant enrichment, particularly antigen processing and presentation pathways, including endogenous peptide display via major histocompatibility complex (MHC) class I machinery. These patterns indicate that tamoxifen-refractory MCF-7 populations exhibit increased lipid biosynthetic capacity and enhanced antigen-processing function.

Conversely, repressed transcripts showed predominant enrichment in mitochondrial functional categories, including mitochondrial translation and mitochondrial gene expression programs, as shown in Figure 1b. Additional suppression affected cellular responses to metallic ions (copper and cadmium) and to estradiol. Collectively, these observations suggest coordinated attenuation of mitochondrial translational apparatus alongside diminished estrogen-responsive signaling in treatment-resistant populations.

The KEGG pathway interrogation further delineated pathway-level perturbations accompanying tamoxifen resistance. Induced meta-DEGs demonstrated significant enrichment in antigen processing and presentation, natural killer cell-mediated cytotoxicity, and phagosomal pathways, as shown in Figure 2a. Several immunopathological conditions-including type 1 diabetes, viral myocarditis, and graft-versus-host reactions-were also enriched, reflecting shared immunoregulatory mechanisms. Additionally, steroid biosynthesis and biliary secretion pathways were overrepresented, reinforcing the metabolic rewiring observations from the ontology assessment.

Among repressed transcripts, only two KEGG pathways were statistically significant: FoxO signaling and Hippo signaling, as shown in Figure 2b. Both pathways represent established modulators of cellular proliferation, programmed death, and stress adaptation. Suppression of these tumor-restraining circuits suggests mechanistic pathways by which treatment-resistant cells circumvent proliferative constraints and apoptotic execution.

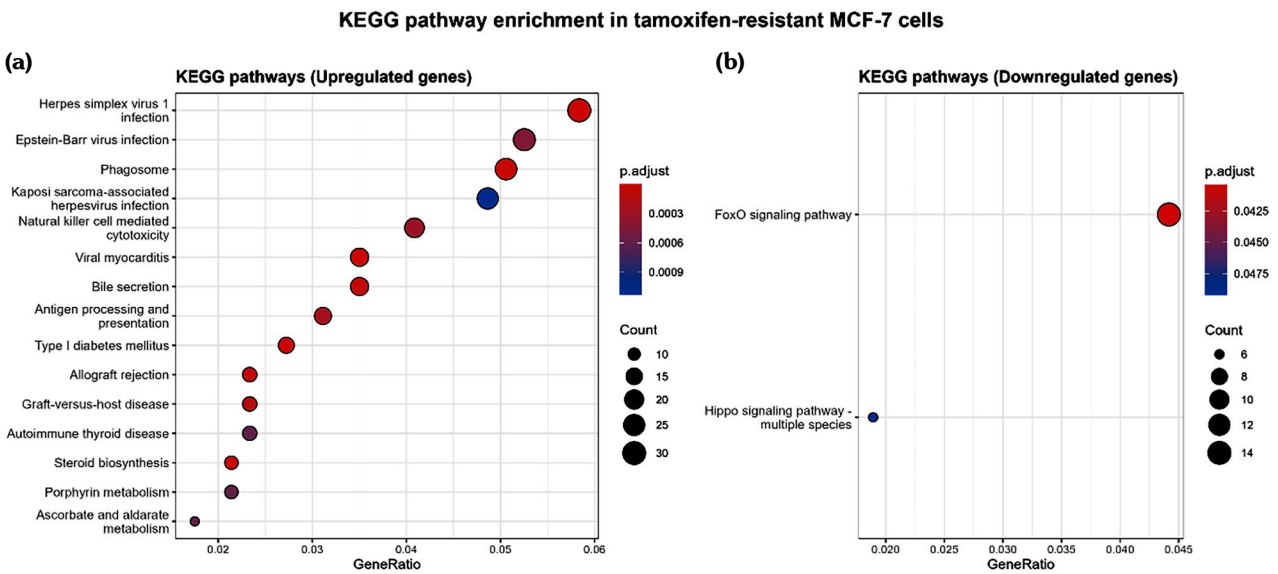

Figure 2. KEGG pathway enrichment analysis of upregulated and downregulated meta-differentially expressed genes in tamoxifen-resistant MCF-7 cells. Combined dot plots show significantly enriched KEGG pathways in upregulated **(a)** and downregulated **(b)** gene sets. Dot size indicates the number of genes mapped to each pathway, and color intensity reflects the adjusted p-value. Upregulated genes are enriched in immune-related pathways, including antigen processing and presentation, natural killer cell-mediated cytotoxicity, and phagosome formation, as well as steroid biosynthesis pathways. In contrast, downregulated genes are selectively enriched in growth-suppressive signaling pathways, notably the FoxO and Hippo signaling pathways.

KEGG: Kyoto Encyclopedia of Genes and Genomes; FoxO: Forkhead box O; MCF-7: Michigan Cancer Foundation-7.

Reactome pathway evaluation provided supplementary mechanistic insight into transcriptional alterations associated with treatment resistance. Induced transcripts showed significant enrichment in cholesterol biosynthetic pathways, SREBP sterol regulatory element binding transcription factor 1 (SREBF1)-mediated cholesterol biosynthesis regulation, and SREBP-driven transcriptional activation, as shown in Figure 3a. Additional enrichment encompassed vascular endothelial growth factor (VEGF) signaling, ER-phagosomal pathways, and MHC class I-mediated antigen presentation, indicating coordinated metabolic, angiogenic, and immunological adaptations. Repressed transcripts showed pronounced enrichment in Reactome pathways governing mitochondrial translational initiation, elongation, and termination, as shown in Figure 3B, with additional suppression of metal-ion-binding and response pathways.

Collectively, GO, KEGG, and Reactome assessments consistently demonstrate that tamoxifen resistance in MCF-7 populations is characterized by: *(i)* induction of cholesterol and steroid biosynthetic pathways driven by SREBP-mediated transcriptional activation, *(ii)* engagement of antigen processing and immunological pathways potentially reflecting modified tumor-immune dynamics, *(iii)* suppression of mitochondrial translational and gene expression programs indicating compromised mitochondrial protein synthesis, and *(iv)* attenuation of FoxO and Hippo signaling suggesting erosion of growth-suppressive regulatory mechanisms. These coordinated transcriptional shifts indicate that metabolic and mitochondrial remodeling constitute fundamental features of tamoxifen resistance.

Among identified meta-DEGs, the lncRNA H19 exhibited consistent dysregulation across independent datasets. Given its established function as a post-transcriptional regulatory hub and genomic template for miR-675, the H19/miR-675 axis was prioritized for experimental corroboration. Moreover, pathway enrichment analyses spanning lipid metabolism,

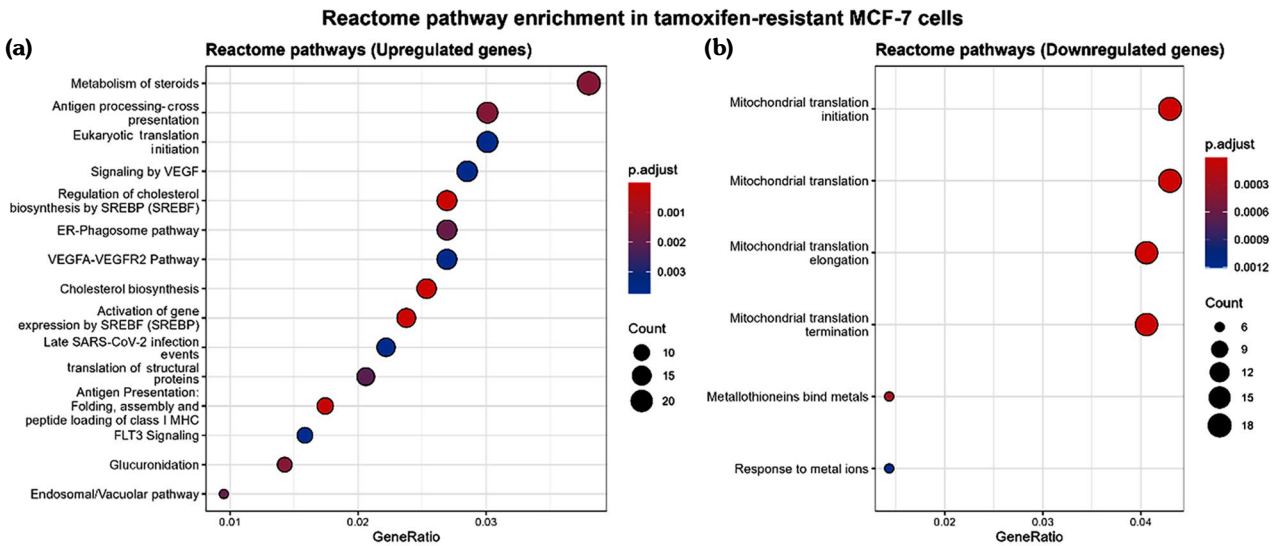

Figure 3. Reactome pathway enrichment analysis reveals metabolic activation and mitochondrial suppression in tamoxifen-resistant MCF-7 cells. Reactome pathway enrichment analysis of meta-differentially expressed genes is shown for upregulated **(a)** and downregulated **(b)** gene sets. Dot plots display enriched Reactome pathways, with dot size indicating gene count and color intensity denoting adjusted p-values. Upregulated pathways include cholesterol biosynthesis, SREBP-mediated transcriptional regulation, and immune-related antigen presentation processes. Conversely, downregulated pathways are primarily associated with mitochondrial translation and protein synthesis, indicating suppression of mitochondrial function in tamoxifen-resistant cells.

MCF-7: Michigan Cancer Foundation-7; VEGF: Vascular endothelial growth factor; SREBP: Sterol regulatory element-binding protein; ER: Estrogen receptor; VEGFA: Vascular endothelial growth factor A; VEGFR2: Vascular endothelial growth factor receptor 2; SARS-CoV-2: Severe Acute Respiratory Syndrome Coronavirus 2; MHC: Major histocompatibility complex; FLT3: Fms Related Receptor Tyrosine Kinase 3.

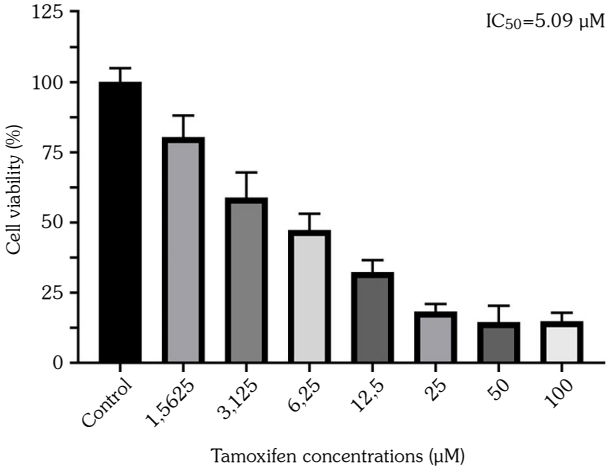

Figure 4. IC_{50} determination of tamoxifen in MCF-7 cells. MCF-7 cells were treated with increasing concentrations of tamoxifen (0-100 µM) for 48 h, and cell viability was measured. Data are presented as mean ± SD of three independent experiments. The IC_{50} value was calculated by nonlinear regression analysis.

MCF-7: Michigan Cancer Foundation-7.

mitochondrial function, and immune regulation suggested extensive remodeling of the regulatory RNA network in resistant populations, providing robust biological justification for investigating H19-centered non-coding RNA interactions at the cellular level.

Tamoxifen cytotoxicity profiling establishes experimental conditions for molecular validation

Tamoxifen's inhibitory effects on MCF-7 viability were characterized to establish working concentrations for molecular investigations. Cellular exposure to escalating tamoxifen concentrations (0-100 µM) over 48 h resulted in concentration-dependent attenuation of viability, as shown in Figure 4. Nonlinear regression modeling of concentration-response relationships yielded a half-maximal inhibitory concentration of 5.09 µM, which was adopted for subsequent experimental procedures.

Experimental validation confirms H19/miR-675-centered ceRNA remodeling following tamoxifen exposure

To empirically corroborate key regulatory elements identified by computational analysis, quantitative amplification was performed on MCF-7 populations following 48-h tamoxifen exposure at the IC_{50} concentration (5 µM).

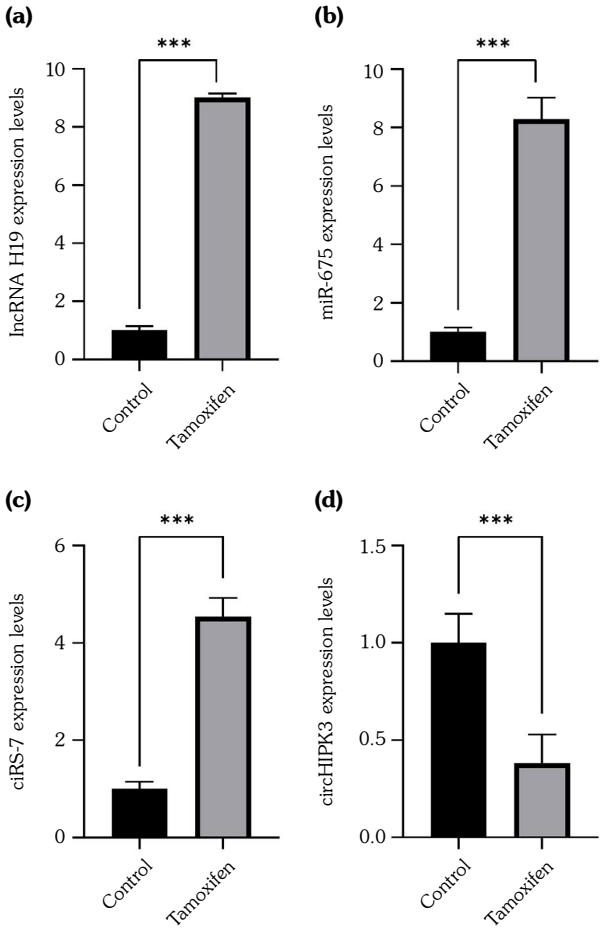

Figure 5. qPCR experiment of the H19/miR-675-centered regulatory network in tamoxifen-treated MCF-7 cells. MCF-7 cells were treated with tamoxifen at its IC_{50} concentration (5 µM) for 48 h. Relative expression levels of lncRNA H19 **(a)**, miR-675-5p **(b)**, ciRS-7 **(c)**, and circHIPK3 **(d)** were quantified by real-time qPCR.

lncRNA: Long non-coding ribonucleic acid; miR: microRNA; ciRS: circRNA sponge; circHIPK: Circular homeodomain-interacting protein kinase; qPCR: Quantitative polymerase chain reaction; MCF-7: Michigan Cancer Foundation-7; RNA: Ribonucleic acid. Data are presented as mean ± SD from three independent experiments. Statistical significance was determined using Student's t-test ($p<0.001$).

Transcript levels of lncRNA H19, its derivative miR-675-5p, and circRNAs ciRS-7 and circHIPK3 underwent quantification relative to untreated controls.

Amplification analysis demonstrated robust induction of the lncRNA H19 ($p<0.001$) and miR-675-5p ($p<0.001$) in tamoxifen-challenged populations, confirming activation of the H19/miR-675 axis. Concurrently, ciRS-7 exhibited marked upregulation ($p<0.001$), whereas circHIPK3 abundance declined substantially ($p<0.001$), as shown in Figure 5a-d.

These findings collectively demonstrate that tamoxifen challenge induces coordinated ceRNA network reprogramming in MCF-7 populations, characterized by activation of the H19/miR-675 signaling axis, enhanced circRNA-mediated miRNA sequestration via ciRS-7, and circHIPK3 suppression. This regulatory reconfiguration supports a mechanistic framework in which tamoxifen-challenged cells remodel the post-transcriptional regulatory architecture to promote survival and adaptive signaling.

DISCUSSION

Endocrine resistance remains a major clinical challenge in ER+ breast cancer, and accumulating evidence indicates that metabolic adaptation and non-coding RNA–mediated regulation play central roles in this process. In this study, integrative transcriptomic analyses across multiple independent datasets revealed consistent alterations in lipid metabolism, mitochondrial function, and post-transcriptional regulatory networks in tamoxifen-resistant MCF-7 cells. Together, these observations suggest that tamoxifen resistance is not driven by a single pathway but rather arises from coordinated molecular reprogramming.

One of the most consistent features identified across datasets was the enrichment of lipid and sterol metabolic pathways, particularly those related to cholesterol biosynthesis. Experimental studies have shown that tamoxifen-resistant breast cancer cells exhibit pronounced lipid metabolic rewiring, which supports membrane dynamics and enables estrogen-independent survival signaling.[13,14] Cholesterol accumulation has also been proposed to function as an alternative growth-promoting factor under endocrine pressure. In line with these reports, our findings indicate that lipid metabolic activation coincides with suppression of mitochondrial translation and gene expression, suggesting a shift away from mitochondrial-dependent energy regulation toward a more adaptable metabolic state.

Alongside this, downregulation of FoxO and Hippo signaling pathways was observed, both of which are known to restrain proliferation and promote apoptotic responses. Loss of these growth-suppressive pathways has been linked to reduced sensitivity to endocrine therapy and enhanced cellular survival. The combined suppression of mitochondrial function and tumor-suppressive signaling supports the idea that tamoxifen-resistant cells adopt a survival-oriented phenotype that favors adaptability over metabolic efficiency.

In addition to metabolic remodeling, our results highlight a coordinated reorganization of non-coding RNA networks following tamoxifen exposure. The lncRNA H19 and its derivative miR-675 were markedly induced, consistent with previous reports demonstrating that H19 contributes to tamoxifen resistance through autophagy activation and epigenetic regulation.[8,9] Induction of miR-675 further supports the involvement of this axis in adaptive transcriptional responses under endocrine stress.

Notably, circRNAs displayed divergent regulation. Upregulation of ciRS-7 suggests enhanced sequestration of tumor-suppressive miRNAs during tamoxifen challenge, whereas circHIPK3 expression was reduced. While circHIPK3 has been implicated in therapy resistance in other settings, its downregulation here may reflect context-dependent regulation or differences between acute drug exposure and stable resistance states. Indeed, previous studies have demonstrated that circRNA-mediated ceRNA networks can directly modulate tamoxifen sensitivity in breast cancer cells.[15,16]

However, the present study has certain limitations. Experimental validation was conducted exclusively in the ER+ MCF-7 breast cancer cell line, which, although widely used as a canonical model of endocrine-responsive disease, may not fully reflect the biological heterogeneity of ER+ breast cancer. Consequently, the extent to which these findings can be generalized to other ER+ models or to endocrine-resistant patient-derived systems remains to be determined. Moreover, although our integrative analyses and experimental validation reveal coordinated alterations in the H19/miR-675/circRNA regulatory network following tamoxifen exposure, the associations identified herein are predominantly correlative in nature. While the observed transcriptional changes are consistent with previously reported mechanisms of endocrine resistance, causal relationships

between the H19-centered regulatory axis and tamoxifen resistance cannot be definitively established within the scope of the present study. Accordingly, future investigations incorporating targeted functional perturbation approaches and *in vivo* model systems will be essential to delineate the mechanistic contributions of this network and to evaluate its clinical relevance.

In conclusion, these findings suggest that tamoxifen exposure triggers early, coordinated metabolic and post-transcriptional adaptations that may precede the establishment of stable endocrine resistance. The convergence of lipid metabolic activation with H19-centered regulatory remodeling underscores interconnected mechanisms that could serve as early indicators of treatment adaptation and potential therapeutic targets.

Data Sharing Statement: The data that support the findings of this study are available from the corresponding author upon reasonable request.

Author Contributions: E.Y., Ö.A.: Idea/concept, design, analysis and/or interpretation; Ö.A.: Control/supervision, critical review; E.Y.: Data collection and/or processing, literature review, writing the article, references and fundings, materials.

Conflict of Interest: The authors declared no conflicts of interest with respect to the authorship and/or publication of this article.

Funding: The authors received no financial support for the research and/or authorship of this article.

REFERENCES

1. Bray F, Laversanne M, Sung H, Ferlay J, Siegel RL, Soerjomataram I, et al. Global cancer statistics 2022: GLOBOCAN estimates of incidence and mortality worldwide for 36 cancers in 185 countries. CA Cancer J Clin 2024;74:229-63. doi: 10.3322/caac.21834.
2. Bullock M. FOXO factors and breast cancer: Outfoxing endocrine resistance. Endocr Relat Cancer 2016;23:R113-30. doi: 10.1530/ERC-15-0461.
3. Yan Y, Zhang J. Mechanisms of tamoxifen resistance: Insight from long non-coding RNAs. Front Oncol 2024;14:1458588. doi: 10.3389/fonc.2024.1458588.
4. Zhang H, Yan C, Wang Y. Exosome-mediated transfer of circHIPK3 promotes trastuzumab chemoresistance in breast cancer. J Drug Target 2021;29:1004-15. doi: 10.1080/1061186X.2021.1906882.
5. Siemińska I, Lenart M. Immunometabolism of innate immune cells in gastrointestinal cancer. Cancers (Basel) 2025;17:1467. doi: 10.3390/cancers17091467.
6. Brindisi M, Fiorillo M, Frattaruolo L, Sotgia F, Lisanti MP, Cappello AR. Cholesterol and mevalonate: Two metabolites involved in breast cancer progression and drug resistance through the ERRα pathway. Cells 2020;9:1819. doi: 10.3390/cells9081819.
7. Fernández-Suárez ME, Daimiel L, Villa-Turégano G, Pavón MV, Busto R, Escolà-Gil JC, et al. Selective Estrogen Receptor Modulators (SERMs) affect cholesterol homeostasis through the master regulators SREBP and LXR. Biomed Pharmacother 2021;141:111871. doi: 10.1016/j.biopha.2021.111871.
8. Wang J, Xie S, Yang J, Xiong H, Jia Y, Zhou Y, et al. The long noncoding RNA H19 promotes tamoxifen resistance in breast cancer via autophagy. J Hematol Oncol 2019;12:81. doi: 10.1186/s13045-019-0747-0.
9. Sun H, Wang G, Cai J, Wei X, Zeng Y, Peng Y, et al. Long non-coding RNA H19 mediates N-acetyltransferase 1 gene methylation in the development of tamoxifen resistance in breast cancer. Exp Ther Med 2022;23:12. doi: 10.3892/etm.2021.10934.
10. Vennin C, Spruyt N, Dahmani F, Julien S, Bertucci F, Finetti P, et al. (2015). H19 non-coding RNA-derived miR-675 enhances tumorigenesis and metastasis of breast cancer cells by downregulating c-Cbl and Cbl-b. Oncotarget 2015;6:29209-23. doi: 10.18632/oncotarget.4976.
11. Rahmati Y, Asemani Y, Aghamiri S, Ezzatifar F, Najafi S. CiRS-7/CDR1as; An oncogenic circular RNA as a potential cancer biomarker. Pathol Res Pract 2021;227:153639. doi: 10.1016/j.prp.2021.153639.
12. Toro-Domínguez D, Martorell-Marugán J, López-Domínguez R, García-Moreno A, González-Rumayor V, Alarcón-Riquelme ME, et al. ImaGEO: integrative gene expression meta-analysis from GEO database. Bioinformatics 2019;35:880-2. doi: 10.1093/bioinformatics/bty721.
13. Hultsch S, Kankainen M, Paavolainen L, Kovanen RM, Ikonen E, Kangaspeska S, et al. Association of tamoxifen resistance and lipid reprogramming in breast cancer. BMC Cancer 2018;18:850. doi: 10.1186/s12885-018-4757-z.
14. Simigdala N, Gao Q, Pancholi S, Roberg-Larsen H, Zvelebil M, Ribas R, et al. Cholesterol biosynthesis pathway as a novel mechanism of resistance to estrogen deprivation in estrogen receptor-positive breast cancer. Breast Cancer Res 2016;18:58. doi: 10.1186/s13058-016-0713-5.
15. Sang Y, Chen B, Song X, Li Y, Liang Y, Han D, et al. circRNA_0025202 regulates tamoxifen sensitivity and tumor progression via regulating the miR-182-5p/FOXO3a axis in breast cancer. Mol Ther 2019;27:1638-52. doi: 10.1016/j.ymthe.2019.05.011.
16. Li H, Li Q, He S. Hsa_circ_0025202 suppresses cell tumorigenesis and tamoxifen resistance via miR-197-3p/HIPK3 axis in breast cancer. World J Surg Oncol 2021;19:39. doi: 10.1186/s12957-021-02149-x.